

# UC Santa Barbara

## UC Santa Barbara Previously Published Works

### Title

An automatic variogram modeling method with high reliability fitness and estimates

### Permalink

<https://escholarship.org/uc/item/39732412>

### Authors

Li, Zhanglin  
Zhang, Xialin  
Clarke, Keith C  
[et al.](#)

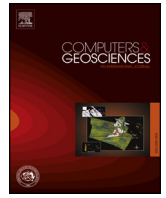
### Publication Date

2018-11-01

### DOI

10.1016/j.cageo.2018.07.011

Peer reviewed



# An automatic variogram modeling method with high reliability fitness and estimates

Zhanglin Li<sup>a,b,\*</sup>, Xialin Zhang<sup>a,b</sup>, Keith C. Clarke<sup>c</sup>, Gang Liu<sup>a,b</sup>, Rui Zhu<sup>c</sup>

<sup>a</sup> Computer School, China University of Geosciences, Wuhan, 430074, China

<sup>b</sup> Hubei Key Laboratory of Intelligent Geo-Information Processing, China University of Geosciences, Wuhan, 430074, China

<sup>c</sup> Department of Geography, University of California, Santa Barbara, CA, 93117, USA

## ARTICLE INFO

### Keywords:

Variogram modeling  
Experimental variogram  
Ordinary kriging  
Variogram fitting  
Genetic algorithm

## ABSTRACT

Modeling of the variogram is a critical step for most geostatistical methods. However, most of the prevalent variogram-based solutions are designed without sufficient consideration of the effect of the interpolation process on their application. This paper proposes an automated variogram modeling framework, which simultaneously considers the fit of the experimental variogram and interpolation accuracy in the modeling variogram interpolation result. The variogram modeling framework can be treated as a nonlinear optimization problem with two sub-goals. The first is to optimize the goodness of fit between the experimental and theoretical variogram values under the conditions of their designated parameters. Second, we seek to optimize the difference between measured values and the associated kriging estimates with the candidate variogram model. A typical case study was chosen using a public dataset to test the proposed method, which was implemented using a genetic algorithm, and its performance was compared with the ones of other commonly applied variogram modeling approaches. As expected, the traditional variogram modeling method that only considers fitting standard experimental variograms showed severe sensitivity to errors in data and parameters; classical cross-validation modeling results tended to overlook the experimental variograms. By contrast, the proposed method succeeded in producing variogram models with robust, high-quality kriging estimates and favorable fitness of experimental variograms in a more powerful and flexible way.

## 1. Introduction

For most geostatistical methods, a critical step to measuring the spatial structure or relationships for data of interest is modeling of the variogram, which has been a research focus in this field for a long-time. Maximum likelihood and least squares are the two common ways to achieve this model fitting goal.

Maximum likelihood (ML) methods, which estimate the variogram model parameters by minimizing a negative log-likelihood function under a multi-Gaussian assumption, are gaining ground among geostatisticians, especially when used to incorporate trends and external drift (Mardia and Marshall, 1984; Oliver and Webster, 2014; Pardo-Igúzquiza et al., 2009). An attractive feature of this method is that the variogram parameters are directly calculated and obtained without intermediate steps. However, an ML estimator is strongly model dependent (Cressie, 1985). It assumes that the data follow a multivariate Gaussian distribution, which is a formidable requirement to fulfill and one that is almost impossible to verify (Kerry and Oliver, 2007).

Furthermore, user-friendly software with enough flexibility to use this method is not common in the public domain. Thus, although the ML method has a valuable role to play in variogram modeling, it is not a widespread approach in practice and will not be considered in this research.

By contrast, the method of least squares (LS) has become a standard means of objective variogram modeling, with certain computational simplicity and broad availability to be implemented within geostatistical software packages. Oliver and Webster (2014) argued that LS approach should be satisfactory if applied with understanding in 90% of all geostatistical investigations.

LS variogram modeling is regarded as an indirect method since calculation of experimental variograms (also known as the sample variogram or empirical variogram) is required. In this procedure, the most frequently used estimator is the method of moments (Matheron, 1965), which is nonparametric and has many favorable properties, such as unbiasedness and consistency in a pointwise sense (Miranda and Souto De Miranda, 2011).

\* Corresponding author. Computer School, China University of Geosciences, Wuhan, 430074, China.

E-mail address: [lizhl@cug.edu.cn](mailto:lizhl@cug.edu.cn) (Z. Li).

<https://doi.org/10.1016/j.cageo.2018.07.011>

Received 4 January 2018; Received in revised form 6 July 2018; Accepted 31 July 2018

Available online 10 August 2018

0098-3004/ © 2018 Elsevier Ltd. All rights reserved.

The main process of variogram modeling with the LS method is to fit discrete experimental variogram values with the closest negative definite function model. To achieve this goal, first a valid variogram model should be chosen and then its corresponding parameters evaluated using LS criteria.

The LS variogram parameter estimates are those that minimize the squared differences between the theoretical model and the experimental variogram. Currently, there are several different kinds of LS methods, among which ordinary least squares (OLS), weighted least squares (WLS) and generalized least squares (GLS) are commonly known. Among the three methods, OLS is the simplest; GLS offers more statistical efficiency at the price of more complexity since it takes into account correlation between variogram estimators at different lags (Cressie, 1985); and WLS can be regarded as a compromise between the OLS and GLS criteria (Lahiri et al., 2002). Since it is simple to implement and efficient in application (McBratney and Webster, 1986; Miranda and Souto De Miranda, 2011; Zimmerman and Zimmerman, 1991), WLS is the most widely accepted among the three methods.

More recent studies (Han et al., 2016; Oliver and Webster, 2014) have shown that the WLS method yields the most satisfactory results in fitting a variogram model. The classical and most commonly used WLS method was proposed by Cressie (1985). Based on the principles of WLS, a series of improved automated machine-learning methods have been proposed recently, such as simulated annealing and nonlinear least squares (Emery, 2010), iterative least squares (Desassis and Renard, 2013), genetic programming and support vector machines (Han et al., 2016).

Most of these methods have been developed to directly fit a model to one or more experimental variograms. However, variogram modeling is rarely an isolated goal. In most cases, its ultimate objective is to estimate data values at un-sampled locations. Besides, It is notable that the main objective of variogram modeling is to capture the major spatial features of the attribute, not to build a variogram model that is the closest possible to experimental values (Goovaerts, 1997). Using these machine-learning approaches, without exception the variogram modeling result can perfectly fit the experimental variogram values under the ideal calculation conditions. Yet in practical applications, the effect of the variogram model used in estimation remains unknown to some extent.

Besides the ML and LS methods, it is notable that variogram identification can also be accomplished by cross-validated statistics (Kitanidis, 1991; Lebel and Bastin, 1985; Samper and Neuman, 1989). As in the systematic illustration of this method by Lebel and Bastin (1985), it is based on the assumption that the parametric variogram model is only an approximation of the true-field variogram; this is a realistic point of view (in hydrology) since in most practical applications very simple (often isotropic) models are adopted. By contrast, the problem of spatial continuity in geology is commonly much more complicated. Despite the validity, in theory, there are few applications of this method in geological contexts. This interpolation-based variogram modeling method, however, indicates that adequately incorporating the minimization of kriging accuracy into the LS modeling process is essential and feasible.

Therefore, we propose an integrated optimization objective taking both the experimental variogram fit and the interpolation accuracy into account. The basic idea of this research is to insert an explicit constraint mechanism for producing high-quality estimates into the currently used LS variogram modeling method. The main principle and the high quality of the variogram modeling result by using this method will be discussed and illustrated in the case study. First, we discuss the method itself and its implementation.

## 2. Method

We propose an optimal variogram modeling mechanism that simultaneously considers spatial structure and its accompanying

interpolation accuracy. The goal of the method is to minimize the following expression:

$$\theta^* = \arg \min_{\theta \in D} \{w_F O_F(\theta) + w_I O_I(\theta)\} \quad (1)$$

- $\theta$  is a vector containing all of the parameters in a certain variogram model to be evaluated. For instance, for the typical isotropic spherical model with a nugget, the vector  $\theta$  could consist of the following four parameters: nugget value, the model type (“spherical”, for instance), range value and sill value. For implementation in practice, different basic model types can be expressed as a series of discrete variables; for instance, 0 and 1 can be representative of the type of the spherical and the exponential models, respectively;
- $O_F(\theta)$  stands for the goodness of fit, which is the difference between the experimental variogram values and the corresponding theoretical variogram model, as determined by parameter vector  $\theta$ ;
- $O_I(\theta)$  represents the kriging interpolation accuracy by applying the current variogram model parameterized by vector  $\theta$ ;
- $w_F$  and  $w_I$  are weights to adjust the contributions of  $O_F(\theta)$  and  $O_I(\theta)$  to the total optimization goal, respectively;
- $D \subset \mathbb{R}^N$  and  $N$  is the total number of parameters in the vector  $\theta$ .

Common measurements used in estimation, such as mean error (ME), mean squared error (MSE), root mean squared error (RMSE), and the mean squared deviation ratio (MSDR, which is the mean of the squared errors divided by the corresponding kriging variances (Oliver and Webster, 2014)), can be applied individually or in combination for estimating  $O_I(\theta)$  in Eq. (1). Two classic ways to calculate these metrics are cross-validation and jackknifing.

$O_F(\theta)$  can be implemented by similar metrics, such as ME, MSE and RMSE. However, it is important to distinguish which sample value is more or less important while fitting experimental variograms. The sum of weighted squared errors is thus suggested for  $O_F(\theta)$ .

$w_F$  and  $w_I$  can be predefined according to the exploratory data or background analysis in the study area. They should be generally greater than 0.0 to keep the validity of the constraints on experimental variogram fitting and cross-validated estimation. In extreme situations, either  $w_F$  or  $w_I$  could be equal to 0.0 so that the proposed method degenerates into the LS or cross-validation based method.

The optimization criterion in Eq. (1) is straightforward since the accuracy of experimental variogram fitting and interpolation was established several decades ago in the early monographs in geostatistics (Goovaerts, 1997). Also, it is worth noting that the two sub-objects,  $O_I(\theta)$  and  $O_F(\theta)$  in Eq. (1), should be expressed in the same order of magnitude. Normalization or weighting can be used to achieve this goal.

## 3. Case study

### 3.1. Test dataset

This case study was executed based on the Walker Lake Dataset (Isaaks and Srivastava, 1989). The total number of data points in this dataset is 1270, with 780 estimated points and 490 sample points on a two-dimensional grid as shown in Fig. 1. The accompanying summary statistics of the sample and estimated dataset are listed in Table 1, from which it is observed that there are apparent statistical differences between these two datasets. For instance, the mean and variance of the sample dataset are 435 and 89 929, but only 283 and 62 773 for the estimated dataset. These differences, not uncommon in practice, indicate that the sample dataset is not well representative of the whole study area, resulting in potential difficulty in variogram modeling and high-precision interpolation.

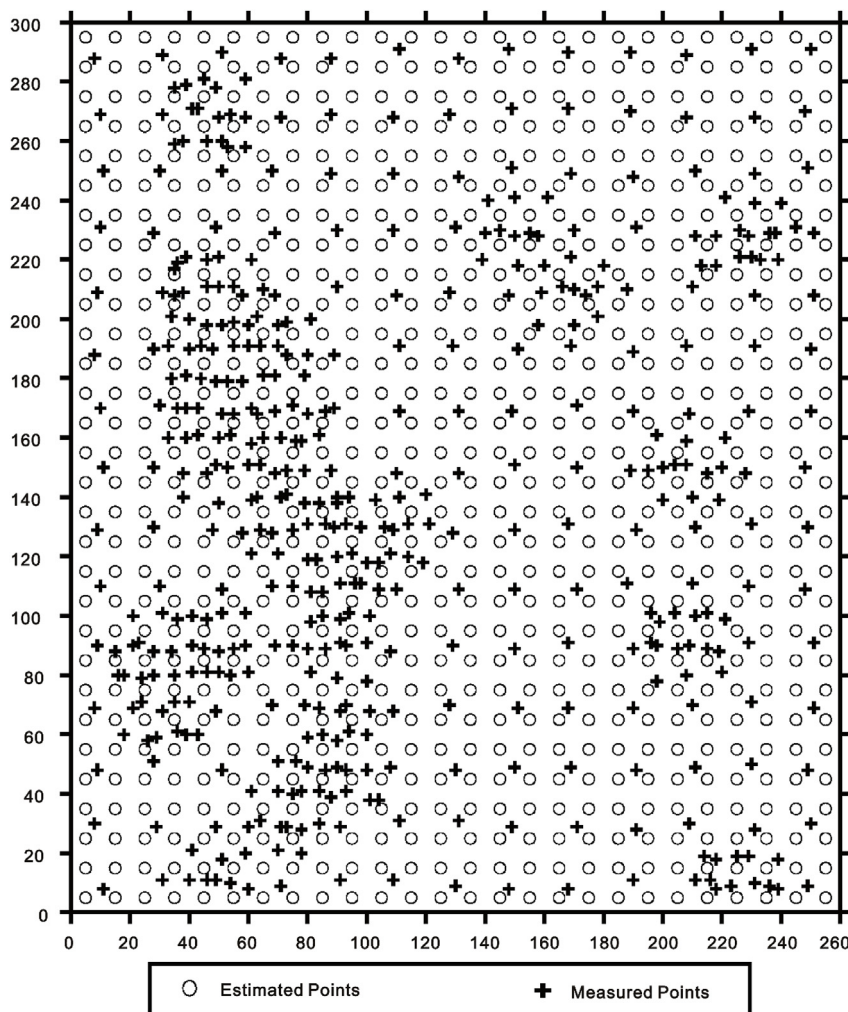


Fig. 1. The position map of the estimated and sample points.

### 3.2. An alternative implementation

#### 3.2.1. Genetic algorithm

As shown in Eq. (1), minimizing inaccuracy both in experimental variogram fitting and interpolation in a multi-dimensional space is a challenging task. A valuable solution to this kind of optimization problem is to use a genetic algorithm (GA), an efficient and robust heuristic tool for searching solutions to optimization problems that has been successfully used in various applications (Clarke, 2017; Villegas-Jiménez and Mucci, 2010). An extensive description of GAs is that by Goldberg (1989).

#### 3.2.2. Objective function

Following Eq. (1), we employed a relative RMSE, which consists of the common RMSE divided by a constant standard deviation, to measure both the experimental variogram goodness of fit  $O_F(\theta)$  and interpolation accuracy for kriging estimates  $O_I(\theta)$ .

As a result,  $O_F(\theta)$  is modeled as:

$$O_F(\theta) = \frac{1}{\sigma_E} \sqrt{\frac{1}{N} \sum_{i=1}^N w(\mathbf{h}_i) [\hat{\gamma}(\mathbf{h}_i) - \gamma(\mathbf{h}_i; \theta)]^2} \quad (2)$$

where  $N$  represents the number of lags applied in calculating the experimental variogram under the associated search conditions;  $\gamma(\mathbf{h}_i; \theta)$  and  $\hat{\gamma}(\mathbf{h}_i)$  respectively stand for modeling and experimental variogram values that corresponds to the  $i$ -th lag under a specific search condition;  $\theta$  stands for the vector of the current candidate parameters for calculating the model values;  $\sigma_E$  is the standard deviation of the whole experimental variogram values used in the fit, and  $w(\mathbf{h}_i)$  is the weight to mark how important the  $i$ -th squared difference between two variogram values is. Cressie (1985) and Pardo-Igúzquiza (1999) provided several alternatives to estimate this parameter, and the following expression is assumed in this study:

$$w(\mathbf{h}_i) = [n(\mathbf{h}_i)]^2 \quad (3)$$

where  $n(\mathbf{h}_i)$  is the number of contributing sample pairs for the  $i$ -th lag  $\mathbf{h}_i$ .

For the measurement of interpolation accuracy,  $O_I(\theta)$ , it is similarly

Table 1

Summary statistics of the sample and estimated points.

Dataset name	Data count	Mean	Variance	Maximum	Upper quartile	Median	Lower quartile	Minimum
SamplePots.dat	470	435.30	89929.40	1528.10	639.50	423.40	184.40	0
EstimatedPots.dat	780	283.00	62772.81	1322.52	444.64	218.45	70.27	0

expressed as:

$$O_I(\theta) = \frac{1}{\sigma_S} \sqrt{\frac{1}{M} \sum_{k=1}^M [\hat{z}(k) - z(k; \theta)]^2} \tag{4}$$

where  $z(k; \theta)$  and  $\hat{z}(k)$  are respectively the estimated value and the measured value for the  $k$ -th point;  $M$  is the total number of the sampled points; and  $\sigma_S$  is the standard deviation of the sampled values in the interpolation.  $O_I(\theta)$  in this study was estimated by cross-validation.

In this implementation, the sum of  $w_F$  and  $w_I$  in Eq. (1) is required to be 1.0. According to this constraint and Eqs. (2)–(4), the final objective function is:

$$O(\theta) = \frac{1.0 - w_I}{\sigma_E} \sqrt{\frac{1}{N} \sum_{i=1}^N [n(\mathbf{h}_i)]^2 [\hat{\gamma}(\mathbf{h}_i) - \gamma(\mathbf{h}_i; \theta)]^2} + \frac{w_I}{\sigma_S} \sqrt{\frac{1}{M} \sum_{k=1}^M [\hat{z}(k) - z(k; \theta)]^2} \tag{5}$$

### 3.2.3. Chromosome representation

The typical encoding mechanism based on binary strings was applied in this research. For convenience and flexibility, a complete chromosome was built by transforming the optimized parameters in the vector  $\theta$  of Eq. (5) into corresponding genes in order. Fig. 2 shows the full chromosome pattern in the case where all of the variogram parameters in a simple two-dimensional variogram model are required to be optimized. It is worth noting that the variogram model type is the only discrete parameter in the chromosome, where the three commonly used basic variogram models (spherical, exponential and Gaussian) plus nugget are prepared to be evaluated and selected in this case study. The corresponding discretization formula representing the type of basic models is listed as follows:

$$\text{Model type} = \begin{cases} \text{Spherical} & , 0 \leq T < 1 \\ \text{Exponential} & , 1 \leq T < 2 \\ \text{Gaussian} & , 2 \leq T < 3 \end{cases} \tag{6}$$

where  $T$  is the gene value representing the type of basic model in the chromosome.

Note that this encoding pattern is dynamic and its gene can be automatically increased or decreased according to any ad hoc problems. For instance, if the main anisotropy angle is known and does not need to be optimized, its corresponding gene can be removed from the chromosome. In order to visually illustrate the variogram modeling and comparison results concisely, however, only the classical nugget plus a single model were considered in the case study.

### 3.2.4. Algorithm implementation

The algorithm has been implemented as a plug-in of the Stanford Geostatistical modeling Software SGeMS (Remy et al., 2011), which is a flexible and extendable geostatistical package. The GA with a crowding mechanism provided in GALib, which is a classic C++ library of GA components (Wall, 1996), is highly efficient in this application and therefore was selected for the following test.

Key algorithms employed in the experiment consist of calculating the objective function and performing the GA-based primary optimization process.

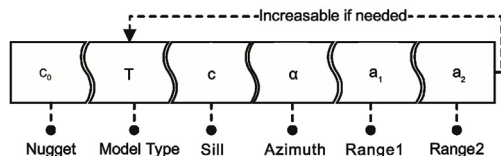


Fig. 2. Chromosome dynamic coding for variogram modeling with a two-dimensional theoretical model.

### Algorithm 1: objective function calculation.

- (1) Decode the current genome to obtain the candidate variogram model;
- (2) Read the basic experimental variogram data, calculate the corresponding variogram model values and evaluate its goodness of fit;
- (3) Execute the cross-validation and assess the interpolation errors;
- (4) Calculate and return the objective value based on the two kinds of errors from steps (2) and (3).

### Algorithm 2: primary optimization process.

- (1) Read the related parameters such as the GA mutation and cross probability;
- (2) Initialize population and evaluate every individual gene by calculating the objective value and the associated fitness score;
- (3) Sequentially execute the genetic operators (selection, crossover, mutation) to generate a new population;
- (4) Re-evaluate the new population. If the termination criterion is not satisfied, continue to evolve by performing steps (3)–(4); if yes, stop and execute step (5);
- (5) Decode the best genome and output the optimized variogram model.

Detailed procedures and the relationship between these two algorithms are shown in Fig. 3.

### 3.3. Test parameters and methods

For an objective comparison of the calculation process and its result, the classical WLS and cross-validation based methods (Lebel and Bastin, 1985) were selected and also implemented using a GA in the case study.  $O_F(\theta)$  in Eq. (2) was employed as an objective function to perform the traditional WLS method;  $O_I(\theta)$  in Eq. (4) was applied as an optimization goal to implement the classical cross-validated method. Also, for the convenience of comparison, the traditional WLS and cross-validation based methods are respectively termed the fitting-oriented (FO) and interpolation-oriented (IO) method; and, accordingly, the proposed method is termed the fitting and interpolation-oriented (FIO) method.

In the test,  $w_I$  in Eq. (5) was assigned to 0.5 by default such that  $O_F(\theta)$  and  $O_I(\theta)$  could play an equally important role in the proposed method. Additionally, we also elaborated on a special sensitivity analysis on this parameter in section 3.7. In order to obtain experimental variograms for the modeling process, a set of typical parameters was designed and is shown in Table 2, with the details of calculations plotted in Fig. 7.

Based on the computed experimental variograms, the FO, IO and FIO methods with the GA were executed in sequence to evaluate the spatial structure of the sample data. Since GA itself was not the focus of this experiment, the GA parameters were fixed for the three methods as follows: the maximum number of generations at 200; the population size was assigned as 200; and the crossover probability and mutation probability were set as 1.0 and 0.01, respectively. In addition, to ensure the repeatability of the experiment, all tests used a random seed for the GA set to a constant of 1, except for the special test on varied random seeds.

For the sake of evaluating the full ability of the proposed method, we suppose that any other prior information for the study area is unknown except for the measured values of samples. According to the spatial distribution, summary statistics and the calculated experimental variogram of the sample dataset, all of the variogram parameters need to be evaluated within their maximum ranges of possible valid values as described in Table 3. An additional condition to this table is that the sum of the sill and nugget should be equal to the global variance of the sample data, which is commonly regarded as the theoretical sill in variogram modeling (Gringarten and Deutsch, 2001).

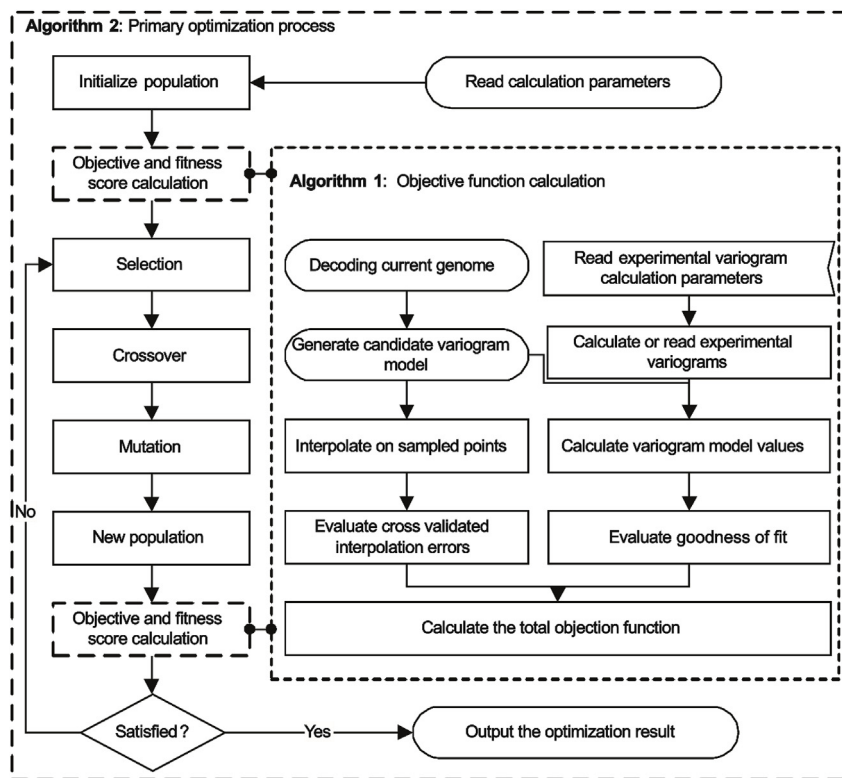


Fig. 3. Block diagram of the GA based algorithm implementation.

Since the search neighborhood will significantly affect kriging estimates and determine which part of the variogram model will be applied while interpolating, a series of search parameters, as shown in Table 4, were sequentially tested to obtain an appropriate neighborhood model. The corresponding variogram modeling results, with these varied search neighborhoods by the FIO method, were surprisingly similar to each other; their anisotropy angles were around 160° and thus can be plotted in Fig. 4. These resulting anisotropy angles are also consistent with other FIO modeling results in the following test contexts (e.g., Fig. 6 and Fig. 9). Conversely, the IO method presents significant instabilities in this context.

Thus it can be concluded that the FIO method was not sensitive to search neighborhood parameters in this study. So as to be able to compare our results with the work of Isaaks and Srivastava (1989), all of the samples within 25 m of the estimated point were adopted for ordinary kriging (OK) in the cross-validation and actual interpolation process.

### 3.4. Test with different GA random seeds

An issue in complex multi-parameter optimization, is the difficulty for GA to repeatedly produce the same consequence. This characteristic can be evaluated for a stability test of the three variogram modeling methods. Here a random seed set consisting of 12 constants (1, 2, ..., 12) was used in sequence with GA to produce different variogram modeling results.

Table 2  
Parameters for calculating reference experimental variograms in four directions.

No.	Azimuth (°)	Dip (°)	Angle tolerance (°)	Lag count	Lag distance (m)	Lag tolerance (m)	Band (m)
(1)	0	0	22.5	20	10	5.0	50
(2)	45	0	22.5	20	10	5.0	50
(3)	90	0	22.5	20	10	5.0	50
(4)	135	0	22.5	20	10	5.0	50

Table 3  
Valid value ranges of parameters to be evaluated.

Parameter Type	The corresponding value range
Nugget(m)	[0, 50000]
Model type	Spherical; Exponential; Gaussian
Sill(m)	[0.00001, 120000]
Range1(m)	[10, 200]
Range2(m)	[10, 200]
Azimuth (°)	[0, 180]

Table 4  
A series of neighborhood parameters for the FIO method.

No.	The range of participated sample count	Search radius(m)
(1)	[1, 20]	200
(2)	[1, 40]	200
(3)	[1, 60]	200
...	...	...
(10)	[1, 200]	200
(11)	[1, 200]	20
(12)	[1, 200]	40
(13)	[1, 200]	60
...	...	...
(20)	[1, 200]	200

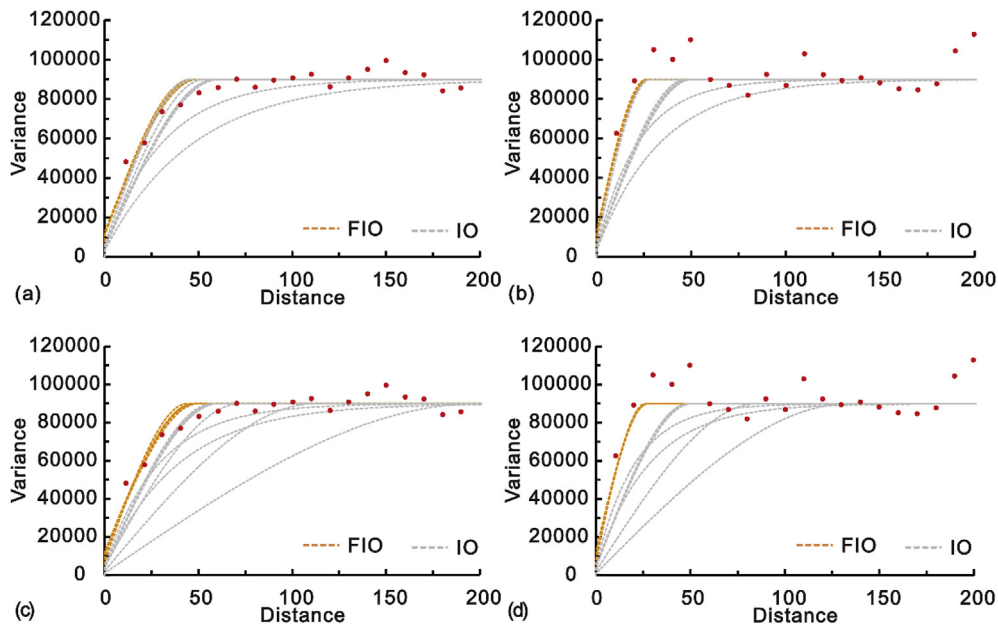


Fig. 4. The experimental variogram vs. the FIO and IO variogram modeling results with neighborhood parameters in Table 5; (a) 160° and (b) 250° for parameters (1)–(10); (c) 160° and (d) 250° for parameters (11)–(20).

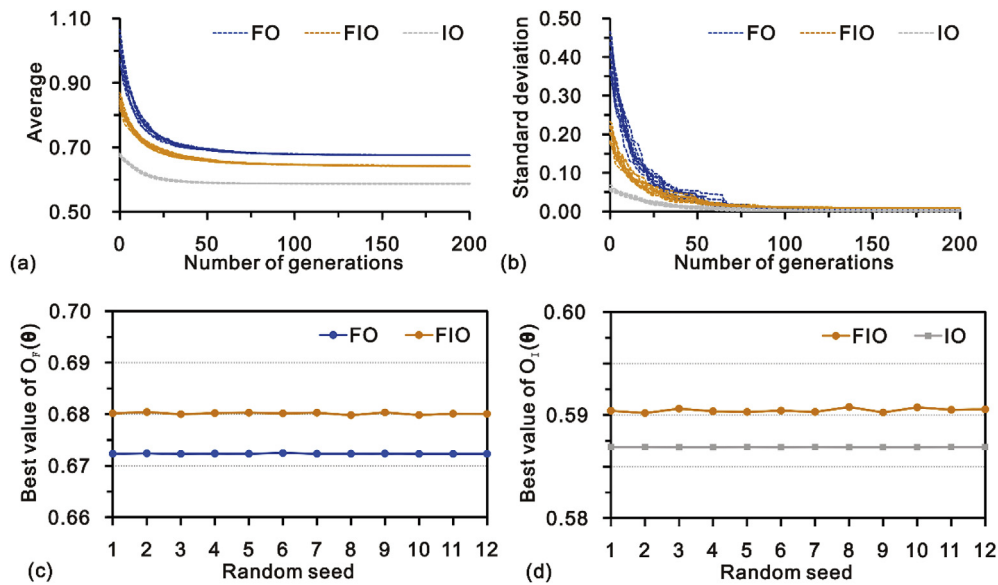


Fig. 5. (a) Average and (b) standard variance of the objective function values vs. the number of generations in evolutions with 12 different random seeds for the FO, FIO and IO method; the objective value of the best individual in experimental variogram fitting (c) and cross-validation (d).

Fig. 5 shows that the GA evolution process for the three methods (the FO, FIO and IO), is relatively stable and consistent in the case of 200 initial individuals with different random seeds. Although there are some differences in their evolution efficiencies, they both succeeded in achieving considerable convergence after 200 iterations. As shown in Fig. 5c–d, both  $O_F(\theta)$  and  $O_I(\theta)$ , in Eq. (2) and Eq. (4), respectively, from the FIO method are greater than, but very close to, the corresponding results from the FO and IO methods for all of the 12 random seeds.

Fig. 6a shows that most of anisotropy angles of the modeling results for the three methods with varied random seeds are around 160° and therefore the resulting models can be observed in this direction. As shown in Fig. 6b–c, the result differences among the three methods for different random seeds are significant. The FO models have large nuggets and unstable main ranges compared with the FIO models;

however, they both fit the experimental variograms well. By contrast, the IO results are relatively more different from the experimental variogram values. The distinctions between the FIO models and the results generated by the other two methods are caused by balancing the requirements of fitting the experimental variograms and producing high-accuracy estimates.

The goodness of fit between the reference experimental variograms (calculated by the search parameters in Table 2) and the modeling results from the three methods is shown in Figs. 7 and 8a in a qualitative and quantitative way, respectively. Both the FIO and FO produced satisfactory results with respect to the fit of the experimental variograms; the IO method, however, yielded disappointing variogram models. For example, as shown in Fig. 8a, the average RMSE for the FO, FIO and IO method were 8 196, 8 291 and 28 778, respectively.

Another kind of GA optimization result is the interpolation accuracy

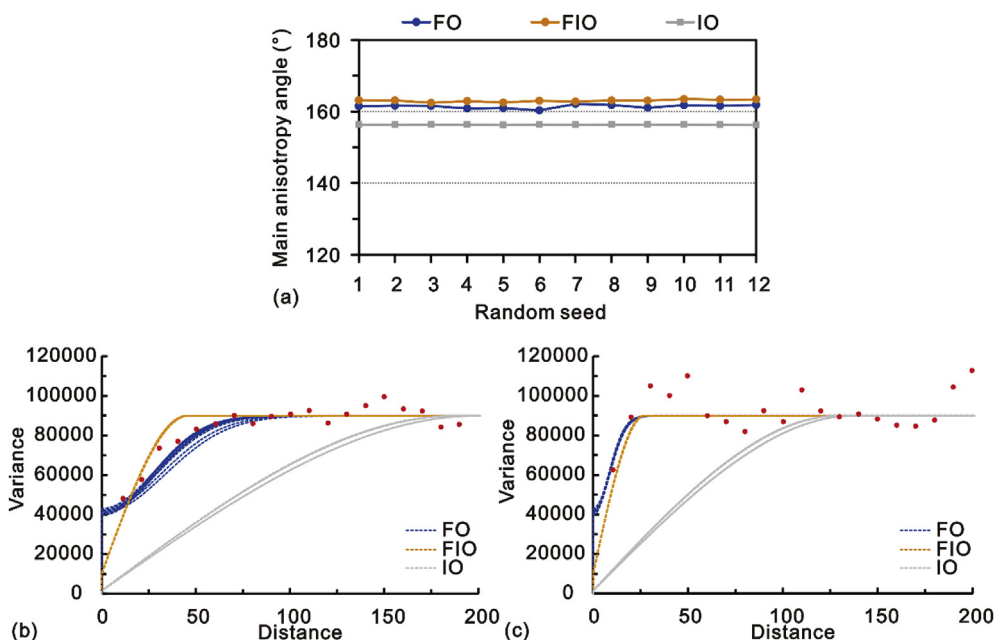


Fig. 6. (a) The main anisotropy directions of the modeling results by the FO, FIO and IO methods with 12 random GA seeds; and the corresponding models vs. the experimental variograms along (b) and perpendicular to (c) the mean of main anisotropy directions (160°).

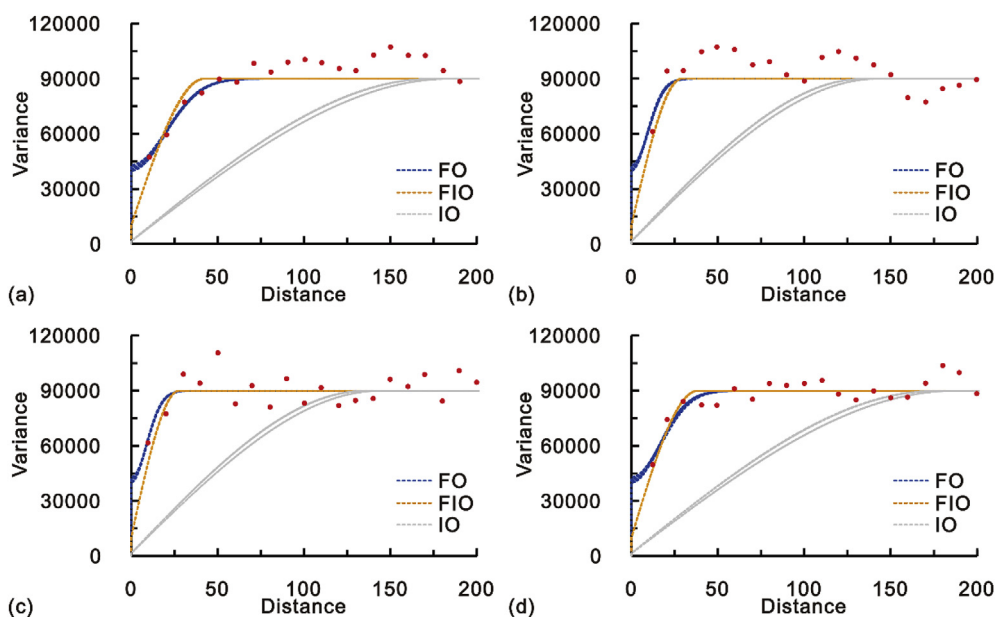


Fig. 7. The FO, FIO and IO variogram modeling results with 12 random GA seeds vs. the experimental variograms in the reference four directions; (a) 0° (b) 45° (c) 90° and (d) 135°.

of cross-validation. With control over the estimation quality, it is predictable that the FIO and IO methods will produce lower cross-validated interpolation errors than the FO method. This prediction is verified by Fig. 8b, in which the FIO and IO models produced estimates with similar accuracy measured by RMSE; in comparison, the FO models failed to yield such accurate estimates.

In the actual interpolation process, OK with the three different kinds of variogram model results was executed in order, with the accompanying interpolation accuracy measured by RMSE as described in Fig. 8c. Interpolation accuracy of the estimates by the FIO and IO method is clearly superior to that for the FO method. For all the cases where random seeds vary from 1 to 12, the mean of the RMSEs from the FO method is 152.90, whereas the corresponding measurement from the FIO and IO method are 144.55 and 144.53. Fig. S1 (in the

Supplementary Material) reveals the estimation details of cross-validation and actual interpolation for the three methods in the case where the random seed is 1.

Comparing and analyzing the differences among the modeling results in Fig. 8, it is notable that the quality of estimates resulting from the same variogram model differs in cross-validation and actual interpolation. For instance, by using the FIO method, the RMSE value was around 177 for cross-validation but reached a much smaller value, 145, for the actual interpolation. A major reason for this difference is that the samples used cannot adequately represent the characteristics of the estimated data. However, this lack of representation in sample dataset, which is not uncommon in practice, does not adversely affect the superiority of the FIO method in interpolation.

It is worth noting that although it is similar among the interpolation

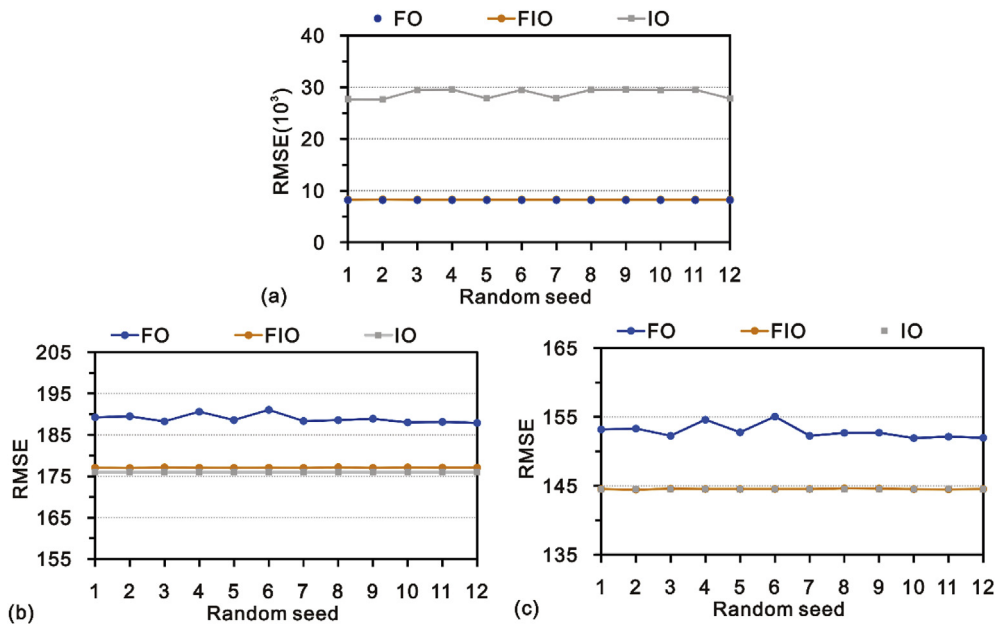


Fig. 8. RMSEs in fitting the reference experimental variograms (a), cross-validation (b) and actual interpolation (c) with the FO, FIO and IO modeling results by the 12 random seeds.

accuracy and goodness of fit when using variograms that are modeled from the proposed FIO method and classic one (Isaaks and Srivastava, 1989); the latter adopts an elaborately nested model and involves both objective and subjective geostatistical steps to obtain the variogram parameters. On the contrary, the FIO just employs a relatively simple model and performs almost the whole modeling process in a fully automated way.

From the above calculation result and corresponding analysis, it can be concluded that the FIO method can produce robust variogram modeling results, with high accuracy both for the fitting of the experimental variograms and actual interpolation estimates.

### 3.5. Test with different numbers of experimental variograms

It is widely accepted that a larger number of experimental variograms will enhance the quality of the variogram modeling results, especially in the case of modeling by eye. However, the number of necessary directions is hard to define. Therefore, it is important to test the sensitivity of variogram modeling on the number and directions of experimental variograms.

As shown in Table 5, 19 search azimuth sets were designed to generate different sets of experimental variograms. All of the azimuth sets are then calculated and applied in the variogram modeling for the FO and FIO method. The corresponding performance analysis in experimental variogram fitting, cross-validation and real estimation is demonstrated in Figs. 9 and 10.

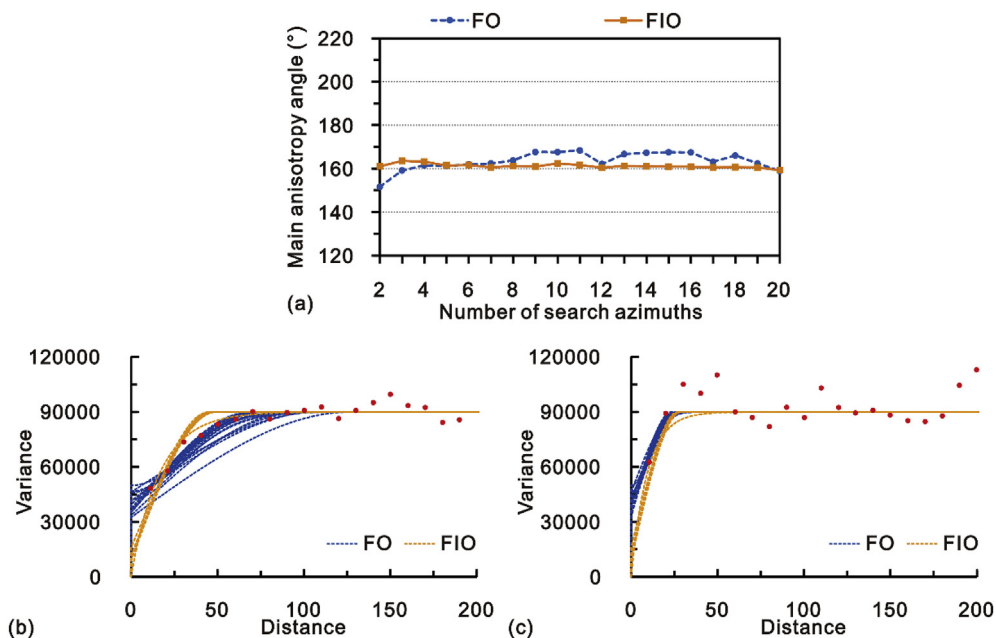


Fig. 9. (a) The main anisotropy directions of the modeling results by the FO and FIO methods with the 19 azimuth sets; and the corresponding models vs. the experimental variograms along (b) and perpendicular to (c) the mean of main anisotropy directions ( $160^\circ$ ).

**Table 5**  
A series of search azimuth sets used for variogram modeling.

Number of azimuths	The corresponding search azimuth set (°)	Angle tolerance(°)
2	0, 90	45
3	0, 60, 120	30
4	0, 45, 90, 135	22.5
5	0, 40, 80, 120, 160	20
...	...	...
20	0, 9, 18, 27, 36, 45, ..., 171	4.5

Fig. 9a shows that the main anisotropy angle varies little and is recognized to be around 160°, except for the case when only two experimental variograms are used in the FO method,. Therefore, all variogram models can be plotted together as in the above situation.

Fig. 9b–c reveal the variogram modeling results of the FO and FIO method in the context of different numbers of experimental variograms. Stability is observed for the FIO variogram models, of which all types of the theoretical model are the spherical except in the case of 20 search azimuths; the max range is around 47 and the min range around 27 with the nugget less than 15 000. On the contrary, either for the types of theoretical model or for the associated parameter values, the FO method produces more uncertain results.

Fig. 10a quantitatively illustrates that the variogram modeling results from both methods match well with the experimental variograms in the corresponding directions. Fig. 10b–c shows that the FIO method succeeded in producing stable, favorable results both in cross-validation and in actual interpolation. From these figures, it is notable that as the number of experimental variograms increases, the FIO method keeps producing kriging estimates with high interpolation accuracy, except for a minor fluctuation in the case when the number of experimental variograms is 20, which means sample pairs within many associated search lags are probably not sufficient for calculating reliable experimental variogram values. For the FO method, however, it is not until the number of experimental variograms falls between 12 and 16 that the corresponding interpolation accuracy relatively stabilizes. Obviously, the FIO method performs significantly better irrespective of the number of experimental variograms used.

**Table 6**  
Random dataset draw from the original sample dataset.

No.	Dataset name	Proportion in original dataset	Number of samples
(1)	S10	10%	47
(2)	S20	20%	94
(3)	S30	30%	141
...	...	...	...
(10)	S100	100%	470

3.6. Test with different numbers of samples

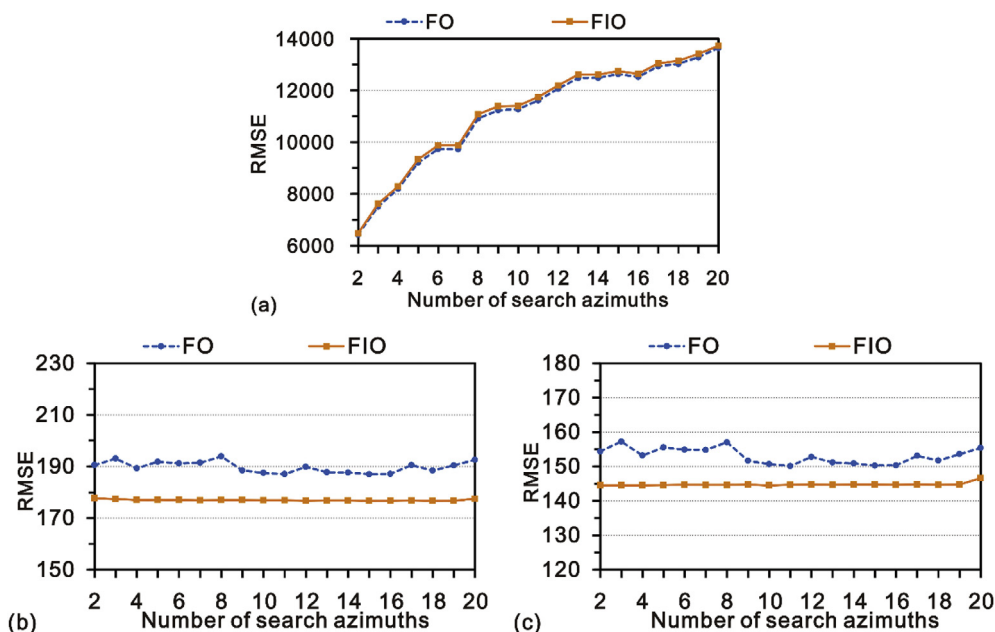
Similar experimental results can also be observed across different numbers of samples. In our study, ten different sample sub-datasets (shown in Table 6), which were randomly drawn as 10%, 20%, ..., 100% of the samples from the original 470 sample dataset, were generated to test the stability of the proposed method.

Fig. 11a presents the calculation time of variogram modeling by the three methods with different sample datasets. Their coefficients of variation of the main variogram parameters are revealed in Fig. 11b, which indicates that results from the FIO method vary relatively slightly compared with these from the other two methods. The details of Fig. 11b can be observed in Table S1a-b in the Supplementary Material.

Fig. 12 shows different accuracies of the three kinds of modeling results in experimental variogram fit and interpolation. As expected, the FO method succeeded in fitting the experimental variograms; the IO method produced favorable cross-validated interpolation accuracy; and the FIO accomplished a favorable balance between the two.

3.7. Test with different cross-validation weights

As the superiority of the FIO method is to consider both the accuracy of fitting experimental variograms and OK interpolation, it is of great significance to elaborate on different FIO modeling results with varied contributions of  $O_I(\theta)$  or  $O_F(\theta)$  in Eq. (5). Thus, a series of cross-validation weights,  $w_1$ , were applied in the FIO modeling in the test dataset. Fig. 13 indicates that the FIO results are relatively stable for weights between 0.1 and 0.9. Fig. 14 shows that a broad range of possible weights, from 0.3 to 0.7, would guide the FIO method to



**Fig. 10.** RMSEs in fitting the reference experimental variograms (a), cross-validation (b) and actual interpolation (c) with the FO and FIO modeling results using the 19 azimuth sets.

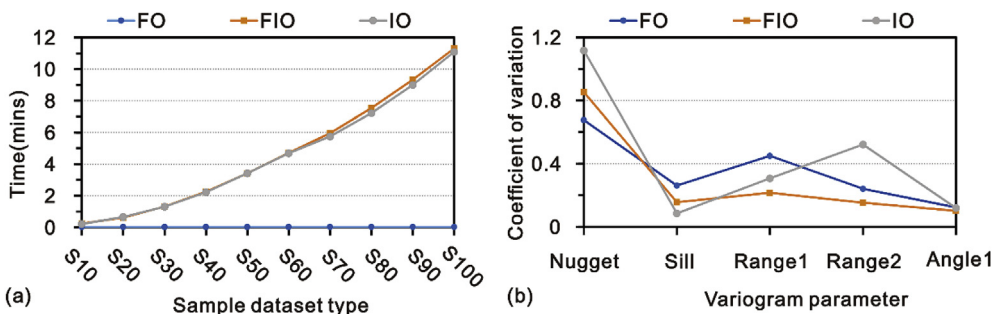


Fig. 11. (a) Calculation times and (b) the corresponding modeling results of the three test methods in variogram modeling for different sample datasets using a desktop with the Intel Core i7 CPU (2.20 GHz).

produce favorable variogram models measured by both experimental variogram fit and OK estimation.

In summary, the IO modeling results generally produced estimates with high accuracy regardless of the experimental variograms; the FO models matched well with the reference experimental variograms, but they were frequently unable to yield favorable estimates. Besides, both of them lacked significant stability in different contexts. By contrast, the FIO method not only produced satisfactory results measured by the goodness of fit of experimental variograms and quality of estimates, but also kept being stable as the calculation parameters varied.

#### 4. Discussion

As shown in Fig. 11a, the FO method is of high efficiency; however, the relative longer computation time for our proposed method is a significant issue. This shortage could be significantly overcome by only keeping the candidate models which fit the experimental variograms well for calculating the complete objection function. However, this process should be performed carefully since valuable solutions might be filtered out by a too strict rule.

In essence, both the FO and IO method share the same goal of revealing the spatial continuity of the data of interest as completely as possible. However, they both depend on a unique constraint (experimental variograms or kriging estimates), which might introduce noticeable uncertainties. Thus, there is not much practical significance to

obtain a “best” model by constraining either on experimental variograms or kriging estimates under a certain set of calculation parameters. Many valuable solutions would be generated by using either the FO or IO method in practice. Suppose  $F$  and  $I$  are the solution sets of variogram models from the FO and IO methods, respectively; few elements in  $F$  and  $I$  that could represent the real spatial continuity will probably belong to the intersection of  $F$  and  $I$ ,  $F \cap I$ , which is rightly corresponding to the solution set of the FIO method. The significant similarity among the FIO results in different contexts in the test implies the validity of this method.

Thus, the proposed method is consistent with classic FO and IO methods; in theory, it will benefit from any improvement to the FO or IO methods. Note that only the classic forms of FO and IO method were employed in the test. Further studies using more robust experimental variograms (Lark, 2000; Miranda and Souto De Miranda, 2011), LS methods and cross-validated residuals (Kitanidis, 1991) are worthwhile to be investigated in future FIO modeling.

#### 5. Conclusions

Although multi-point statistics is currently becoming more and more critical in multiple research fields, variogram modeling is still unavoidable for most geostatistical applications. It is true that there is no best variogram model (Goovaerts, 1997). The proposed method aims at simultaneously producing high-quality experimental variogram

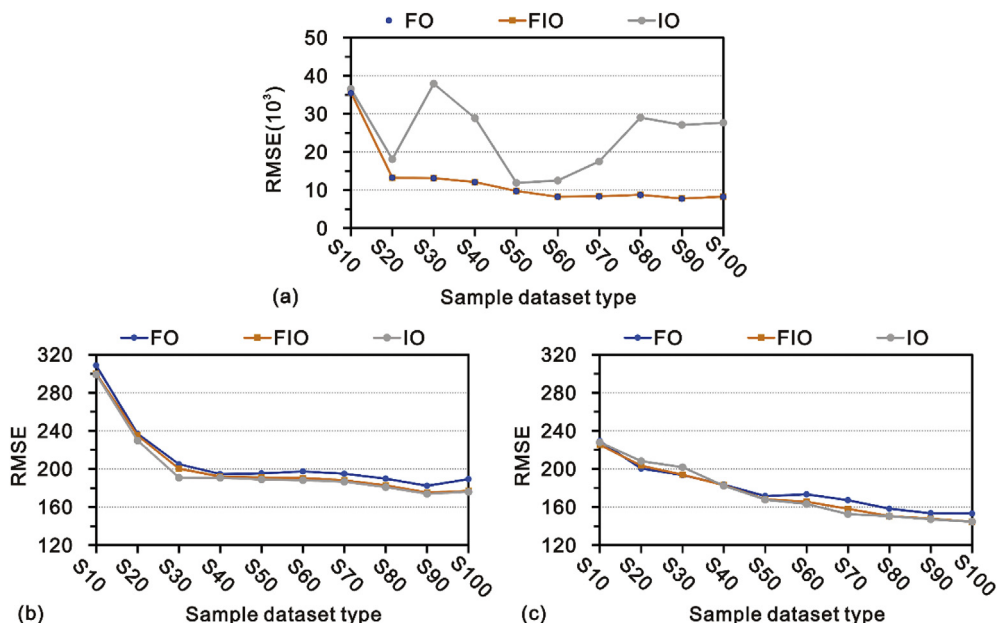


Fig. 12. RMSEs in fitting the reference experimental variograms (a), cross-validation (b) and actual interpolation (c) with the FO, FIO and IO modeling results using the 10 sample dataset.

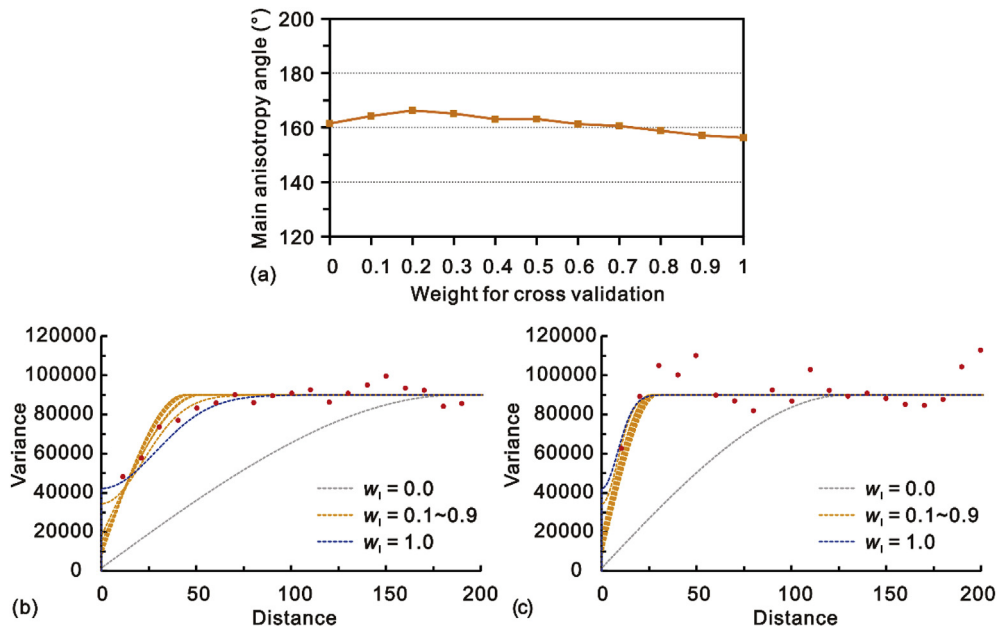


Fig. 13. (a) The main anisotropy directions of the modeling results by the FIO methods with varied weights for cross-validation; and the corresponding models vs. the experimental variograms along (b) and perpendicular to (c) the mean of main anisotropy directions (160°).

fitting and kriging estimates, which are two widely accepted criteria in variogram modeling. The associated implementation, application and superior performance compared with traditional variogram modeling were illustrated by a case study in the paper. According to our findings, we conclude as follows:

- (1) The proposed framework is valid for producing high-quality variogram models in terms of both experimental variogram fitting and actual interpolation; meanwhile, the method is flexible enough to integrate prior knowledge as much as possible and is not sensitive to parameters during implementation, such as the search neighborhood and the reference experimental variograms;
- (2) Cross-validation can be used to evaluate the interpolation accuracy of candidate variogram models and GA is a valuable means to

- implement the proposed method;
- (3) The traditional WLS method is not always able to produce favorable variogram models with respect to the actual interpolation accuracy and the stability of modeling results in the context of varied numbers of experimental variograms or samples.

Nevertheless, it is obvious that the improvement of the proposed method is at the cost of computational time. In the case of a large number of samples, choosing a representative subset of samples, but not the full sample set, would effectively speed up the calculation process. Some parallel computing technologies are also valuable to be implemented in the proposed method. We also conclude that further research is needed in cross-variogram modeling for multi-variable spatial data.

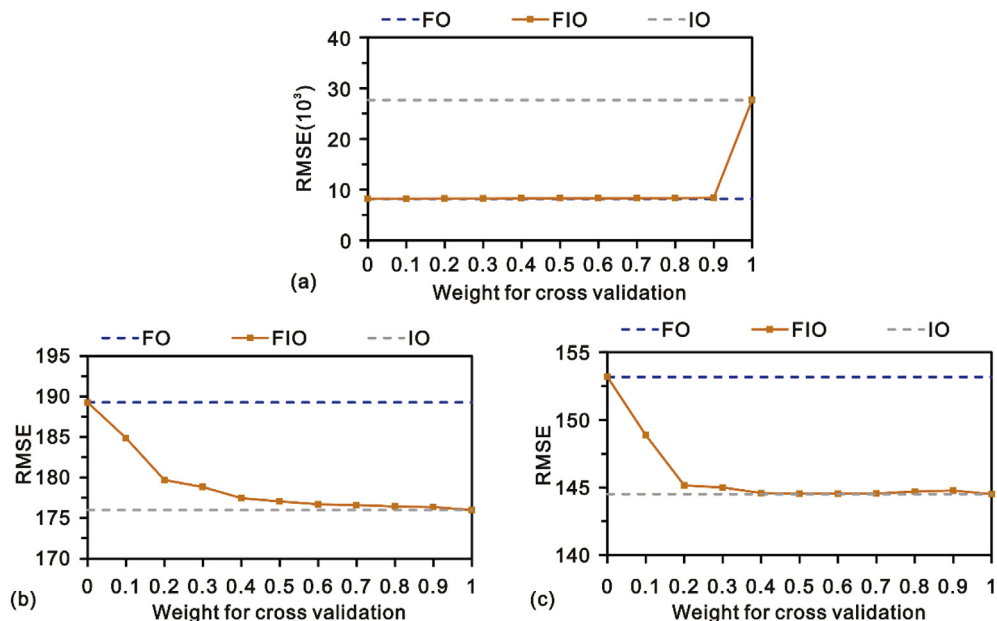


Fig. 14. RMSEs in fitting the reference experimental variograms (a), cross-validation (b) and actual interpolation (c) with the FIO modeling results using the varied weights for cross-validation.

## Acknowledgments

The first author was supported by the National Natural Science Foundation of China (Grant No: 41202231, 41572314 and 61203306). This research was performed while the lead author was on sabbatical at the Department of Geography, University of California, Santa Barbara. The authors are grateful to the editors as well as the reviewers for their helpful and constructive comments.

## Appendix A. Supplementary data

Supplementary data related to this article can be found at <https://doi.org/10.1016/j.cageo.2018.07.011>.

## Statement of authorship

- (1) Zhanglin Li proposed the method, performed analysis on the implementation, interpreted data, wrote manuscript and acted as corresponding author.
- (2) Xialin Zhang helped in improvement of the method in theory, the design and implementation of the algorithm.
- (3) Keith C. Clarke supervised development of work, helped to improve the method in theory, edit and evaluate the manuscript.
- (4) Gang Liu helped to improve the experiment process.
- (5) Rui Zhu helped to edit and improve the manuscript.

An Automatic Variogram Modeling Method with High Reliability Fitness and Estimates.

## References

- Clarke, K.C., 2017. Improving SLEUTH calibration with a genetic algorithm. In: *Proceedings of the 3rd International Conference on Geographical Information Systems Theory, Applications and Management - Volume 1. GAMOLCS. SciTePress, Porto, Portugal*, pp. 319–326.
- Cressie, N., 1985. Fitting variogram models by weighted least squares. *J. Int. Assoc. Math. Geol.* 17, 563–586. <https://doi.org/10.1007/BF01032109>.
- Desassis, N., Renard, D., 2013. Automatic variogram modeling by iterative least squares: univariate and multivariate cases. *Math. Geosci.* 45, 453–470. <https://doi.org/10.1007/s11004-012-9434-1>.
- Emery, X., 2010. Iterative algorithms for fitting a linear model of coregionalization. *Comput. Geosci.* 36, 1150–1160. <https://doi.org/10.1016/j.cageo.2009.10.007>.
- Goldberg, D.E., 1989. *Genetic Algorithms in Search, Optimization, and Machine Learning*. Addison-Wesley Pub. Co., Reading, Mass.
- Goovaerts, P., 1997. *Geostatistics for Natural Resources Evaluation*. Oxford University Press, New York.
- Gringarten, E., Deutsch, C.V., 2001. Teacher's aide variogram interpretation and modeling. *Math. Geol.* 33, 507–534. <https://doi.org/10.1023/A:1011093014141>.
- Han, C., Wang, J., Zheng, M., Wang, E., Xia, J., Li, G., Choe, S., 2016. New variogram modeling method using MGGP and SVR. *Earth Sci. India.* <https://doi.org/10.1007/s12145-016-0251-9>.
- Isaaks, E.H., Srivastava, R.M., 1989. *An Introduction to Applied Geostatistics*. Oxford University Press.
- Kerry, R., Oliver, M.A., 2007. Comparing sampling needs for variograms of soil properties computed by the method of moments and residual maximum likelihood. *Geoderma* 140, 383–396. <https://doi.org/10.1016/j.geoderma.2007.04.019>.
- Kitanidis, P.K., 1991. Orthonormal residuals in geostatistics: model criticism and parameter estimation. *Math. Geol.* 23, 741–758. <https://doi.org/10.1007/BF02082534>.
- Lahiri, S.N., Lee, Y., Cressie, N., 2002. On asymptotic distribution and asymptotic efficiency of least squares estimators of spatial variogram parameters. *J. Stat. Plann. Inference* 103, 65–85. [https://doi.org/10.1016/S0378-3758\(01\)00198-7](https://doi.org/10.1016/S0378-3758(01)00198-7).
- Lark, R.M., 2000. A comparison of some robust estimators of the variogram for use in soil survey. *Eur. J. Soil Sci.* 51, 137–157. <https://doi.org/10.1046/j.1365-2389.2000.00280.x>.
- Lebel, T., Bastin, G., 1985. Variogram identification by the mean-squared interpolation error method with application to hydrologic fields. *J. Hydrol.* 77, 31–56. [https://doi.org/10.1016/0022-1694\(85\)90196-9](https://doi.org/10.1016/0022-1694(85)90196-9).
- Mardia, K., Marshall, R., 1984. Maximum likelihood estimation of models for residual covariance in regression. *Biometrika* 1, 135–146. <https://doi.org/10.1093/biomet/71.1.135>.
- Matheron, G., 1965. *Les Variables Régionalisées et leur Estimation: une Application de la Théorie de Fonctions Aléatoires aux Sciences de la Nature*. Masson et Cie, Paris.
- McBratney, A.B., Webster, R.J., 1986. Choosing functions for semi-variograms of soil properties and fitting them to sampling estimates. *Eur. J. Soil Sci.* 37 [https://doi.org/10.1016/0148-9062\(87\)90683-8](https://doi.org/10.1016/0148-9062(87)90683-8). 617–639.
- Miranda, H., Souto De Miranda, M., 2011. Combining robustness with efficiency in the estimation of the variogram. *Math. Geosci.* 43, 363–377. <https://doi.org/10.1007/s11004-010-9308-3>.
- Oliver, M.A., Webster, R., 2014. A tutorial guide to geostatistics: computing and modeling variograms and kriging. *Catena* 113, 56–69. <https://doi.org/10.1016/j.catena.2013.09.006>.
- Pardo-Igúzquiza, E., 1999. VARFIT: a fortran-77 program for fitting variogram models by weighted least squares. *Comput. Geosci.* 25, 251–261. [https://doi.org/10.1016/S0098-3004\(98\)00128-9](https://doi.org/10.1016/S0098-3004(98)00128-9).
- Pardo-Igúzquiza, E., Mardia, K.V., Chica-Olmo, M., 2009. MLMATERN: a computer program for maximum likelihood inference with the spatial Matérn covariance model. *Comput. Geosci.* 35, 1139–1150. <https://doi.org/10.1016/j.cageo.2008.09.009>.
- Remy, N., Boucher, A., Wu, J., 2011. *Applied Geostatistics with SGeMS: a User's Guide*. Cambridge University Press.
- Samper, F.J., Neuman, S.P., 1989. Estimation of spatial covariance structures by adjoint state maximum likelihood cross validation: 1. Theory. *Water Resour. Res.* 25, 351–362. <https://doi.org/10.1029/WR025i003p00351>.
- Villegas-Jiménez, A., Mucci, A., 2010. Estimating intrinsic formation constants of mineral surface species using a genetic algorithm. *Math. Geosci.* 42. <https://doi.org/10.1007/s11004-009-9259-8>.
- Wall, M., 1996. *GAlib: a C++ Library of Genetic Algorithm Components*. Mechanical Engineering Department, Massachusetts Institute of Technology.
- Zimmerman, D.L., Zimmerman, M.B., 1991. A comparison of spatial semivariogram estimators and corresponding ordinary kriging predictors. *Technometrics* 33, 77–91. <https://doi.org/10.2307/1269009>.